Author/s:
Martig, S;Hitchens, PL;Stevenson, MA;Whitton, RC

Title:
Subchondral bone morphology in the metacarpus of racehorses in training changes with distance from the articular surface but not with age

Date:
2018-06-01

Citation:
Martig, S., Hitchens, P. L., Stevenson, M. A. & Whitton, R. C. (2018). Subchondral bone morphology in the metacarpus of racehorses in training changes with distance from the articular surface but not with age. Journal of Anatomy, 232 (6), pp.919-930. https://doi.org/10.1111/joa.12794.

DR. R. CHRIS WHITTON (Orcid ID : 0000-0003-0012-4065)

Article type : Original Paper

Subchondral bone morphology in the metacarpus of racehorses in training changes with distance from the articular surface but not with age

Sandra Martig[1], Peta L. Hitchens[1], Mark A. Stevenson[2], R. Chris Whitton[1]

Running head: subchondral bone morphology in racehorses

Author affiliation:

[1] The Equine Centre, Faculty of Veterinary and Agricultural Sciences, The University of Melbourne, 250 Princes Highway, Werribee, VIC, 3030, Australia.
cwhitton@unimelb.edu.au

[2] Faculty of Veterinary and Agricultural Sciences, The University of Melbourne, Parkville, Victoria 3010, Australia

Key words: morphology, subchondral bone, micro-CT, metacarpal condyle, racehorse

Abstract

The repetitive large loads generated during high-speed training and racing commonly cause subchondral bone injuries in the metacarpal condyles of racehorses. Adaptive bone modelling leads to focal sclerosis at the site of highest loading in the palmar aspect of the metacarpal condyles. Information on whether and how adaptive modelling of subchondral bone changes during a racehorse's career is sparse. The aim of this cross-sectional study was to describe the changes in subchondral bone micromorphology in the area of highest loading in the palmar aspect of the metacarpal condyle in thoroughbred racehorses as a function of age and training. Bone morphology parameters derived from micro-CT images were evaluated using principal component analysis and mixed-effects linear regression models. The largest differences in micromorphology were observed in untrained horses between the age of 16 and 20 months. Age and duration of a training period had no influence on tissue mineral density, bone volume fraction and number and area of closed pores to a depth of 5.1 mm from the articular surface in 2 to 4-year-old racehorses in training. Horses with subchondral bone injuries had more pores in cross-section than horses without subchondral bone injuries. Differences in bone volume fraction were due to the volume of less mineralised bone. Tissue mineral density increased and bone volume fraction decreased with increasing distance from the articular surface up to 5.1 mm from the articular surface. Further research is required to elucidate the biomechanical and pathophysiological consequences of these gradients of micromorphological parameters in the subchondral bone.

Introduction

Subchondral bone injuries (SCBI) are common in the metacarpal condyles of racehorses and may result in articular surface damage and/or intra-articular fractures (Pinchbeck et al., 2013, Barr et al., 2009, Riggs et al., 1999a) (Muir et al., 2008, Stepnik et al., 2004). As such they pose an animal welfare problem and cause financial losses to the racing industry (Senat, 1991, Trope et al., 2011). These injuries are fatigue injuries that develop as a consequence of the repeated application of large loads generated in the fetlock (metacarpophalangeal) joint during high speed training and racing (Riggs et al., 1999a, Radtke et al., 2003, Whitton et al., 2010, Harrison et al., 2010). Adaptive bone modelling in response to these loads leads to focal sclerosis at the site of highest loading in the palmar aspect of the

metacarpal and metatarsal condyles (Firth et al., 2005, Bogers et al., 2014, Harrison et al., 2010, Riggs and Boyde, 1999). The interaction between this focal sclerosis and subchondral bone injuries is still debated (Norrdin et al., 1998, Riggs et al., 1999a, Whitton et al., 2013, Boyde, 2003). It has been speculated that the gradient of bone volume fraction between sclerotic and non-sclerotic bone may lead to focally increased strains with subsequent damage accumulation (Riggs et al., 1999a). However, sclerosis may be protective as higher bone volume fraction of trabecular bone is associated with increased fatigue resistance (Fatihhi et al., 2015, Rapillard et al., 2006).

In young racehorses bone adapts quickly to the loads of training. The majority of metacarpal diaphyseal new bone in a group of Thoroughbred fillies was produced within the first nine weeks of race training, which included cantering at approximately 8.9 ms^{-1} but not yet galloping at or near racing speed (Boyde and Firth, 2005). A plateau period may be reached after this initial adjustment as subchondral bone mineral density was similar in horses undergoing 18 weeks or 18 months of treadmill exercise but in both groups was higher than in untrained control horses (Firth et al., 1999a, Firth et al., 1999b). The phenomenon of rapid early adaptation of bone to loading followed by a plateau effect is further supported by laboratory experiments. The majority of new bone production in mouse tail vertebrae under cyclic loading occurred within the first ten weeks of loading with little new bone production thereafter, though care is required comparing rodent and equine bone due to the absence of osteonal remodelling in rodents (Lambers et al., 2013).

The morphology of the equine metacarpal condyle has been described in detail but information on how this morphology changes with age and training remains sparse (Rubio-Martinez et al., 2008, Leahy et al., 2010, Riggs et al., 1999b, Boyde et al., 1999). Focal increased bone volume fraction (sclerosis) in the palmar aspect of the metacarpal condyles was associated with closure of smaller marrow spaces and vascular canals (pores) in one study, and increased vascularisation associated with sclerosis and loss of marrow spaces in another study (Boyde and Firth, 2005, Norrdin et al., 1998). Furthermore, the time from rapid early adaptation to training to the plateau phase, and the load required to stimulate this adaptation, is still unknown. Knowledge of these factors would allow safer training of horses at a level where their bones adjust best to the demands of racing.

The aim of this cross-sectional study was to describe the morphology of the palmar aspect of the metacarpal condyle in Thoroughbred racehorses of different ages. We included young untrained horses and trained 2 to 4-year-old horses. We hypothesised that 1) the subchondral bone becomes increasingly sclerotic as a racehorse's career progresses with age; 2) the most dramatic increase in sclerosis occurs within a few weeks of commencing training in the 2 year old horses; 3) tissue mineral density decreases with increasing sclerosis due to the slow process of osteoid mineralisation; 4) the area of pores but not the number decreases with increasing sclerosis due to infilling of existing marrow spaces.

Materials and Methods

Horses

Metacarpal condyles were collected from a convenience sample of Thoroughbred racehorses from Victoria, Australia, that died or were euthanized for reasons unrelated to this study between October 2009 and February 2013. Horses were included if they were 2 to 4-year-old, in race training, did not meet inclusion criteria for other studies which required the metacarpi, and staff were available to collect samples. Furthermore, a convenience sample of 1 and 2- year-old Thoroughbred horses that were bred for racing, but had not yet commenced race training, and died or were euthanized at the University of Melbourne Equine Centre for reasons unrelated to this study, were included as a group of untrained horses.

Fifty horses were included in this study (1-year-old, n = 4; untrained 2-year-old, n = 5; trained 2-year-old, n = 14; 3-year-old, n = 16; 4-year-old, n = 11). There were 25 males (16 castrated), 24 females and one of unknown sex. Causes of death or euthanasia were musculoskeletal stress injury [n = 14; fractured proximal sesamoid bones, fractured humerus (n = 3 each); fractured metacarpal diaphysis, fractured pelvis (n = 2 each); fractured tibia, fractured carpal bones, fractured lateral metatarsal condyle and ipsilateral proximal phalanx and sesamoid bones, fractured metacarpal condyle and contralateral metacarpal diaphysis (n = 1 each)]; trauma related to fast work (n = 1); trauma unrelated to fast work (n = 4); sudden death, exercise induced pulmonary haemorrhage (EIPH), or ruptured major blood vessel (n = 18); anaphylactic reaction (n = 2); gastrointestinal or respiratory disease (n = 7); and cervical vertebral malformation or stenosis (n = 4).

The following information was recorded for each horse: time in training since most recent rest (weeks), number of race starts, and cause of death (euthanasia due to musculoskeletal fatigue injury or other). Subchondral bone injury (SCBI) was graded at post mortem examination by one observer (SM) according to an adaptation of a previously published scheme (Barr et al., 2009). The observer was aware of the horse's cause of death, age and sex at the time of grading. Grading was as follows: 0 (no lesions), 1 (subchondral bone discoloration, normal overlying cartilage), 2 (subchondral bone discoloration and overlaying cartilage lesion) or 3 (subchondral bone and overlying cartilage defect).

Specimen collection

The metacarpi were dissected free from soft tissues. The palmar aspect of the distal condyle was removed with a bandsaw (HT Barnes, BMSS Butchers Machinery, North Coburg, VIC, Australia) by cutting in a proximo-55°palmar-distodorsal oblique plane through the centre of rotation of the condyle. The specimens were wrapped in gauze soaked in saline (0.9% sodium chloride, Baxter, Old Toongabbie, NSW, Australia; or Compound Sodium Lactate [Hartmann's], Fresenius Kabi, Friedberg, Germany), enclosed in ziplock plastic bags, and stored in plastic containers at -20°Celsius (C) until further use and between steps of preparation. Specimens underwent a total of three freeze-thaw cycles between collection and micro-CT image acquisition.

Leg allocation

One leg per horse was selected for the study. For all but two 4-year-old horses only one leg was available. In horses that suffered from a metacarpophalangeal joint injury, the opposite limb was used instead (n = 3). A random number table was used to allocate left or right legs for all other horses as there is little evidence for side predilection for SCBI (Barr et al., 2009, Pinchbeck et al., 2013, White et al., 1977).

Specimen preparation

The lateral condyle was used as it is less commonly and less severely affected by SCBI than the medial condyle (Trope et al., 2011, Tull and Bramlage, 2011, Pinchbeck et al., 2013). The hyaline cartilage was removed with a scalpel blade. A cylindrical specimen with a diameter of approximately 6.7 mm was cut using a diamond coated core drill bit (#102075, Starlite Industries Inc, Rosemont, PA, USA)

mounted on a drill press (3/4 HD 16 Speed Bench Drill Press, Carba-Tec Melbourne Pty Ltd, Springvale, VIC, Australia). Bone cylinders were located 3-5 mm posterior to the transverse ridge and centred in the middle third of the condyle with the cylinder's long axis perpendicular to the articular surface (Fig. 1). The cylinders were cut to a length of 7-8 mm using a diamond coated wavering blade mounted on a low speed saw (IsoMet, Buehler, Lake Bluff, Illinois, USA). Cold tap water was used at all times for cooling and hydration during drilling and cutting.

The specimen of a 3-year-old horse was damaged during drilling, and therefore excluded from analysis.

Micro computed tomography

Image acquisition

Specimens were thawed to room temperature and micro-CT scans were acquired with an *ex vivo* micro-CT scanner (SkyScan 1172, Bruker-microCT N.V., Kontich, Belgium). Specimens were scanned in air in a 5 ml polypropylene tube, held in place with clay so that the specimen long axis was aligned with the scanner axis of rotation. The articular surface was upper most and a drop of physiological saline (Compound Sodium Lactate [Hartmann's], Fresenius Kabi, Friedberg, Germany) was placed onto it to ensure hydration during scanning. Specimen stage temperature reached approximately 27° Celsius during image acquisition resulting in partial evaporation of the saline. The ensuing high humidity in the polypropylene tube maintained specimen hydration while allowing scanning in air.

Images were acquired with a 4.87 µm pixel size, a 2000 x 1333 matrix, 0.5 mm aluminium filter, set x-ray tube potential 70 kV, set tube current 140 µA, rotation step 0.40°, image acquisition over 180°and exposure time of 750 ms resulting in a scan time of approximately 38 min per specimen. Frame averaging was set at 3, and random movement to reduce ring artefact was set at 20. The imaged field of view of approximately 6 mm in length was smaller than the specimen length and chosen to include the entire articular surface and as much of the specimen as possible.

Image reconstruction

Projection images were reconstructed using software provided by the manufacturer (Nrecon version 1.6.6.0, Bruker-microCT, Kontich, Belgium). The following settings were used: dynamic image range min 0 to max 0.156911 attenuation coefficient, ring

artefact reduction 10, beam-hardening correction 51%, and no smoothing. Pixel size remained at 4.87 µm after reconstruction. The software automatically determined misalignment compensation for each specimen individually.

Phantoms of 0.25 g cm^{-3} and 0.75 g cm^{-3} calcium hydroxyapatite (Bruker-microCT, Kontich, Belgium) were scanned, and images reconstructed and filtered (see section *Image analyses*) under the same conditions and software settings as the bone specimens. Images of the phantoms were used to calibrate the software (CTan 1.13.15.1+, Bruker-microCT, Kontich, Belgium) for mineral density calculations.

Image analyses

Multiplanar reconstructions of the images were viewed in three orthogonal planes in custom software (DataViewer 64 bit, version 1.4.4.4, Skyscan, Kontich, Belgium). Images were aligned so that the long axis of the specimen was parallel to the z-axis and assessed for the presence of microcracks, high-density lines at the articular surface, and concentrations of pores within dense bone or concentrations of pores of different size and shape than the surrounding pores. Microcracks were defined as disruption of the normal anatomy by small lucent lines arising from the articular surface at an oblique, usually 45°, angle or a comminuted, saucer-type fracture parallel to the joint surface (Muir et al., 2008, Turley et al., 2014, Williamson et al., 2017). Some of these cracks are filled with highly mineralised tissue and are observed on micro-CT as high-density lines at the articular surface and have been described in equine joints subjected to high loads (Laverty et al., 2015, Williamson et al., 2017, Bani Hassan et al., 2016). These lines can be perpendicular or oblique to the articular surface and may or may not protrude into the hyaline cartilage. Pores consist of marrow spaces separating trabeculae and resorption cavities that are the result of osteoclast activity and of different size and shape than marrow spaces separating tracebulae (Boyde and Firth, 2008). The presence or absence of clusters of the latter was recorded.

Further analysis of the aligned images was performed with proprietary software (CTan 64 bit, 1.13.15.1+, Bruker-microCT, Kontich, Belgium). Three volumes of interest (VOI) were defined in each specimen. VOI diameter was 1092 pixels (5.3 mm) in the centre of the specimen. Volume of interest length was 350 slices (1.7 mm) and all VOIs were contiguous. The distal VOI was chosen to include the distal

most slice that contained articular surface. The VOI diameter of the distal most slices was individually adjusted to accommodate the curvature of the articular surface resulting in slight variation of size of the distal VOI (mean 34.8 μm^3) while all middle and proximal VOIs measured 37.8 μm^3 in size.

Prior to segmentation required for assessment of bone morphometric parameters images were filtered with a median filter in the 3D space using a radius of three pixels. Volumes of interest were thresholded using a global thresholding method in CTAn. The upper range of the thresholding area was set at 255 for all VOIs. The lower end of the range was set subjectively by the same operator (SM) for each specimen and each VOI individually. Specimens were segmented in the same order as for micro-CT image acquisition. For each specimen the distal VOI was segmented first followed by the middle and proximal VOIs. The value for the lower end of the range was chosen for the segmented image to visually best match the original greyscale image. All pixels within the set range of greyscale values were assigned as mineralized bone and all pixels below the lower end of the range were set as background (i.e. pores consisting of marrow spaces and vascular canals).

The following 3D structural parameters were determined with custom software (CTAn, Internal Plug-Ins, 3D analysis): bone volume fraction (BV/TV, in %), specific bone surface (BS/BV in mm^{-1}), bone surface density (BS/TV in mm^{-1}) and tissue mineral density (TMD, in g/cm^3).

The number of closed pores (clporestra) and the area of closed pores (aclporestra in mm^2) in cross-section were determined as 2D parameters. A closed pore is an area of background pixel values (i.e. non-mineralised marrow spaces and vascular canals) that is completely enclosed by mineralised bone. The average value of the 100 distal most slices in each VOI was calculated for both parameters. The 100 distal most slices with maximum diameter were used in the distal VOI.

The original greyscale images were then thresholded again, this time using the two-level Otsu method in CTAn. The lower two-level Otsu thresholding value was replaced with the above used manually determined lower thresholding value for consistency. The upper range of the thresholding area was set at 255 as above. This divided the mineralised bone into highly mineralised and less mineralised bone. The tissue mineral density and volume fraction of the highly mineralised bone (hTMD and

hBV/TV, respectively) and the less mineralised bone (lTMD and lBV/TV, respectively) were determined as above.

Data analyses

The distribution of continuous variables was assessed by examining histograms. Mean and standard deviation were calculated for all micro-CT parameters. Outliers were defined as more than two standard deviations from the mean. To assess whether linear relationships were appropriate, we visually inspected scatter plots between pairs of continuous variables. Linear relationships were deemed appropriate for all relationships between continuous variables without requiring transformation. Box plots of the micro-CT parameters stratified by categorical explanatory variables (e.g. sex) were also generated.

To assess correlations between variables, we performed a principal component analysis (PCA) on the ten micro-CT parameters. The scree test, Kaiser criterion (eigenvalues>1) and proportion of variance were used to determine the number of meaningful principal components. The first three components, accounting for 93.8% of the total variance of the observed variables, were retained for further inspection (Fig. 2). These were component 1 – BV/TV, lBV/TV, BS/BV, and area of closed pores (56.6% of variance); component 2 – TMD, hTMD, and lTMD (26.3%); and component 3 – hBV/TV, BS/TV, and number of closed pores (10.9%). Normally, we would use PCA to reduce the observed micro-CT parameters into a smaller number of principal components (artificial variables); however, this can result in difficulties with interpreting such an artificial variable. Thus, we chose representative variables from each principal component for further analyses: BV/TV (component 1), TMD (component 2), and hBV/TV and number of closed pores (component 3).

The four selected micro-CT parameters (outcome variables) were assessed with mixed effects linear regression models to investigate the effects of the explanatory variables - age, sex, weeks in training since last rest period (grouped into 1 to 9 weeks, 10 to 14 weeks, 15 to 20 weeks, and unknown), number of starts, presence or absence of SCBI, and whether a horse was euthanized because of a musculoskeletal stress injury. A random effects term was included in the model to account for the repeated measures (VOIs) per specimen. Univariable linear

regression was performed for each outcome variable with all explanatory variables. Explanatory variables with $P<0.25$ were included in the initial multivariable model. Variables were then excluded one by one in a step-wise backwards manner and retained if $P<0.05$. Variables excluded during this final step were re-entered into the model one by one and retained in the final model as confounders if they changed the coefficient of a variable in the model by more than 20%. Biologically plausible interactions of variables in the final model were tested one by one and retained in the model if $P<0.05$. The standardised residuals of the final model were tested for normality by visual inspection of the histogram.

Scatterplots of the relationships between BV/TV and TMD as well as number and area of closed pores in cross-section revealed clustering by VOI. Hence, to assess the relationship between these variables linear regression models were fitted, stratified by VOI. Statistical analyses were performed using Stata (Small Stata version 14.2, StataCorp, College Station, TX, USA).

Results

Horses

The three youngest 1-year-old horses in the study (16 to 20 months old) were outliers for multiple parameters. Outliers had lower bone volume fraction and larger pores than the remaining horses (Fig. 3, Table 1). Bone micro-CT morphology parameters for the untrained 2-year-old horses were closer to those of the trained 2-year-old horses than to those of the untrained 1-year-old horses (Table 1). Because of the large differences between untrained 1-year-old and untrained 2-year-old horses and the low numbers of horses in these subgroups, untrained horses were excluded from further statistical analyses.

Of the available trained horses 20 were female, six entire males, 13 castrated males and the sex of one horse was unknown. Mean ± standard deviation of weeks in training was 11 ± 4 (n = 32). Nineteen horses never started in a race and the number of starts was unknown for two horses. Mean ± standard deviation of number of starts for the horses that had at least one start was 7 ± 4 (n = 19). Thirteen horses were euthanized due to musculoskeletal stress injuries.

316

317 **Visual assessment of micro-CT images**

318 Nine horses had grossly visible SCBI within the specimen (grade 1, n = 7; grade 2, n
319 = 2). On micro-CT, seven horses had observable microcracks (Fig. 4B), all of which
320 had SCBI grades > 0. Microcracks consisted of a network of zigzagging cracks in a
321 plane approximately parallel to and 0.5 to 1.5 mm from the articular surface. Six
322 horses had high-density lines at the articular surface (Fig. 4A), five of which also had
323 microcracks. Eight horses had concentrations of pores within dense bone or
324 concentrations of pores of different size and shape than the surrounding pores (Fig.
325 4C).

326

327 **Mixed linear regression of representative variables**

328 Table 2 presents results from the four multivariable mixed-effects linear regression
329 models of factors affecting total bone volume fraction, bone volume fraction of highly
330 mineralized bone, tissue mineral density and number of closed pores.

331

332 In the model predicting bone volume fraction, BV/TV was lower in each VOI with
333 increasing distance from the articular surface.

334

335 In the model predicting tissue mineral density, TMD increased in each VOI with
336 increasing distance from the articular surface. Confounders retained in the final
337 model included whether a horse was euthanized due to a musculoskeletal stress
338 injury, and horses with unknown weeks in training.

339

340 In the model predicting volume fraction of highly mineralized bone, hBV/TV was
341 lower in the distal VOI than in the middle and proximal VOIs but was not different
342 between middle and proximal VOIs (Fig. 5, Table 2). Specifically, hBV/TV was
343 between 45.7% and 55.1% in all horses in the middle and proximal VOIs and in half
344 of the horses also in the distal VOI. The other half of the horses had hBV/TV
345 between 31.0% and 45.1% in the distal VOI, and most of these horses (19 of 20)
346 also had the highest BV/TV (> 96.5%). None of the horses with volume fraction of
347 highly mineralized bone < 42% (n = 16) in the distal VOI had SCBI. When these 16
348 horses were removed, there was no difference in volume fraction of highly
349 mineralized bone between horses with and without SCBI (P = 0.8).

In the model predicting number of closed pores in cross-section, horses with SCBI had more pores in cross-section than horses without SCBI.

Relationship between tissue mineral density and bone volume fraction

A positive correlation was found between bone volume fraction and tissue mineral density in the distal VOI ($R^2 = 0.30$, $P < 0.001$) (Fig. 6). This relationship was also positive for less mineralised bone ($R^2 = 0.45$, $P < 0.001$) but negative for highly mineralised bone ($R^2 = 0.34$, $P < 0.001$). No correlations were found in the remaining VOIs for tissue mineral density (middle VOI: $P = 0.17$; proximal VOI: $P = 0.7$), less mineralized bone (both VOIs: $P = 0.08$) and highly mineralized bone (middle VOI: $P = 0.9$; proximal VOI: $P = 0.5$).

Relationship between area and number of closed pores in cross-section

The relationship between number and area of closed pores in cross-section was positive in the distal ($R^2 = 0.61$, $P < 0.001$), positive in the middle ($R^2 = 0.10$, $P = 0.051$) and negative in the proximal ($R^2 = 0.20$, $P = 0.004$) VOI (Fig. 7).

Discussion

We found that in 2 to 4-year-old thoroughbred racehorses in training, age, duration of training since the last period of rest, and the number of starts had no influence on micromorphology of the subchondral bone up to a depth of 5.1 mm in the palmar aspect of the lateral metacarpal condyle in the area subjected to the highest loading. The largest difference in bone micromorphology was between untrained horses of 20 months of age or less and older untrained horses suggesting adaptation to loading occurs earlier than expected. In horses in training, tissue mineral density increased and bone volume fraction decreased with increasing distance from the articular surface but there was only a weak correlation between these two parameters in the distal VOI and none further away from the articular surface. The amount of highly mineralised bone was similar in all horses in the middle and proximal VOI and half of the horses in the distal VOI. A greater number of closed pores was associated with a larger area of closed pores in the distal VOI, but with a smaller area of closed pores in the proximal VOI. Furthermore, the number of pores remained constant with

increasing distance from the articular surface but horses with SCBI had more pores than horses without SCBI.

There was a lack of influence of age and training on the subchondral bone from the palmar aspect of the mid condylar region of the third metacarpal bone. This is consistent with a previous study where age and cumulative racing activity had limited influence on micromorphology of subchondral bone in Thoroughbred racehorses (Muir et al., 2008). Thoroughbreds at 16 to 20 months of age are still growing, but they are also likely to be transitioned from uncontrolled paddock exercise to the breaker where they undergo limited controlled exercise with a rider as they are educated and possible pre-training where the volume of controlled exercise is gradually increased. We did not account for exposure to the breaker and pre-training because of the low number of horses in the untrained group. The effect of controlled unridden and ridden exercise including breaking-in and pre-training on the bones of foals is controversial. Metacarpal subchondral bone histology and CT appearance were similar in 18-month-old Thoroughbreds whether or not they underwent controlled unridden exercise from the age of three weeks, but age had an influence on volumetric bone mineral density, again independently of whether or not horses underwent controlled exercise (Kawcak et al., 2010, Dykgraaf et al., 2008, Firth et al., 2011). In another study, horses never exposed to the breaker or any training had a lower bone volume fraction in the metacarpal epiphysis than horses exposed to the breaker and race training but it remains unclear at which stage during breaking-in and early race training bone volume fraction increased (Boyde and Firth, 2005). Further research is required to elucidate the natural development of the subchondral bone as horses mature skeletally and how breaking-in and pre-training influences this maturation.

The relationship of increasing tissue mineral density and decreasing bone volume fraction with increasing distance from the articular surface, observed in this study, is similar in horses at different stages of their career. This may not solely be a function of new bone production with initial adaptation to the high loads of racing and training. Periodic high bone turnover has been documented in the distal VOI when the stresses of training are removed during rest periods (Holmes et al., 2014). Contrary to our hypothesis, tissue mineral density was higher with greater bone volume fraction in the distal VOI and there was no correlation between bone volume fraction

and tissue mineral density in the middle and proximal VOIs. The lack of correlation in the middle and proximal VOIs may be due to the small range of values for these parameters in horses in our study, perhaps because the investigated area of subchondral bone had reached maximal adaptation in all study horses in training. Alternatively this absence of a correlation could reflect a lack of power of our study. Well-adapted subchondral bone may reach a plateau of tissue mineral density that no longer changes in relation to bone volume fraction. Further investigation is required to determine the highest biologically possible tissue mineral density in this area of bone.

The bone volume fraction of highly mineralised bone was remarkably similar in the middle and proximal VOI and in half of the horses also in the distal VOI as shown by the lack of horse level effect. This is consistent with a previous study where increasing bone volume fraction was due to infilling of marrow spaces with immature, less mineralised bone suggestive of modelling rather than remodelling of bone (Boyde and Firth, 2005).

We did not expect tissue mineral density to increase with bone volume fraction in the distal VOI. This finding suggests that with increasing bone volume fraction the amount of more mature bone and hence tissue mineral density increases. Interestingly, this increase in tissue mineral density was due to a combination of a large amount of less mineralised bone with a small amount of highly mineralised bone with the tissue mineral density of both less and highly mineralised bone being at the higher end of their respective range found in this study. Increased bone turnover including resorption of highly mineralised bone could explain the presence of a large amount of immature, less mineralised bone (Holmes et al., 2014). This increased bone turnover may have occurred some time prior to sampling to allow both the less and the highly mineralised bone to reach the higher tissue mineral densities observed. Alternatively, other factors such as genetics or nutrition may determine a horse's maximal achievable tissue mineral density. It remains unclear why horses with subchondral bone injuries clustered within the group of horses with more recent remodelling activity in the distal VOI (lower bone volume fraction and tissue mineral density). Further research is required to determine whether this clustering is the cause or the consequence of subchondral bone injuries and whether

achieving a higher bone volume fraction in the distal VOI protects from subchondral bone injuries.

The relationship between the number and area of closed pores in cross-section was complex and different to what we hypothesised. The positive relationship in the distal and middle VOIs may be due to different causes than the negative relationship in the proximal VOI. Image noise, the curved articular surface and the lower tissue mineral density in the distal VOI possibly affect the results of segmentation. Very small pores could reflect image noise rather than true pores. In the proximal VOI, the number of closed pores increased with decreasing area of pores. This may be due to the infilling of larger pores around branching vessels resulting in more but smaller pores in cross-section. Alternatively or additionally, new vascular channels may develop in highly mineralised, mature bone. Furthermore, small resorption spaces associated with remodelling will merge into larger pores once they increase sufficiently in size. In the distal VOI a decrease in size of true very small pores will not lead to more pores because they are already too small to harbour multiple or branching vessels, and is likely to lead to some pores dropping below the spatial resolution of micro-CT resulting in fewer pores.

Horses with SCBI had more pores in the distal VOI than horses without SCBI. Microdamage associated with SCBI may segment as pores and hence artifactually increase the number of pores. Alternatively, targeted remodelling associated with SCBI may result in an increased number of pores representing resorption spaces.

The number of horses with high-density lines in our study is similar to that in a study of thoroughbred racehorses from Hong Kong where the presence of high-density material infills in the subchondral bone and/or mineralised articular cartilage layer was first reported (Boyde et al., 2011). We cannot determine whether the high-density lines in our horses were infills or protrusions as we removed the hyaline cartilage with a scalpel blade prior to micro-CT imaging, which may have fully or partially removed high-density protrusions. Similar high-density material infills and protrusions have also been documented in osteoarthritic third carpal bones in standardbred racehorses, which also undergo high intensity training (Laverty et al., 2015).

Non-mineralised microcracks observed in our specimens were located parallel to the articular surface and did not extend into the articular surface as previously described in micro-CT and microscopic studies (Williamson et al., 2017, Muir et al., 2008, Turley et al., 2014). Removal of the articular cartilage with a scalpel blade may have resulted in removal of some calcified cartilage and hence removal of short oblique fractures in this location. Alternatively, such oblique microcracks may not have been present in our small specimens from the mid-condylar area. Arrangement and location of the microcracks observed in our specimens is similar to the more severe lesions described previously as saucer-type or comminuted fractures parallel to the articular surface with cross-hatched cracks only present at the edge of those lesion (Turley et al., 2014, Muir et al., 2008).

We found no relationship between clusters of pores and other forms of subchondral bone damage. Clusters of pores in sclerotic bone are likely a sign of focal remodelling and have been associated with articular surface defects in equine carpal bones previously (Lacourt et al., 2012). It remains unclear why our finding differed, but as mentioned above the spatial resolution of our micro-CT images could be a limiting factor. Larger numbers of horses and higher resolution imaging are required to further investigate the role of cluster of pores in the pathogenesis of SCBI.

Limitations of this study include the use of a convenience sample, which introduced sampling bias. We believe that this bias was kept to a minimum as exclusion from this study was predominantly due to factors unrelated to the horse. All horses that die or are euthanized on Melbourne metropolitan racetracks are subject to compulsory post mortem exam. Horses from Victorian country racetracks are subject to post mortem exam at the discretion of the attending race steward or veterinarian due to the costs of transport to our facilities. Allocation to other research projects was predominantly based on demand of the project for specimen numbers but occasionally would include a horse of a particular age group. Researcher unavailability for specimen collection was independent of horse death and was kept to a minimum in order to maximise the available number of specimens for this study. The cross-sectional design is another limitation as it relies on different horses providing information on time-varying parameters such as the effect of age and training. A longitudinal study would allow accounting for individual horse level effects when investigating changes over time. However, *ex vivo* micro-CT, with the

advantage of high spatial resolution, would no longer be possible in a longitudinal study and would have to be replaced with high-resolution peripheral quantitative CT (HR-pQCT). The low number of untrained horses and the lack of control of exposure to breaking in and pre-training are further limitations, especially as bone micromorphology seems to change most around the age of 16 to 20 months. Furthermore, the horses in this study came from a large number of different trainers and were exposed to different training regimes and racetrack surfaces. All these factors influence the risk of musculoskeletal injury (Parkin et al., 2004, 2005, Cogger et al., 2006, Verheyen et al., 2006), and have the potential to influence subchondral bone micromorphology. Missing data for the explanatory variables, especially weeks in training, likely reduced the power of our study. The finding that horses with unknown weeks in training since the last period of rest had lower tissue mineral density in all VOIs compared to horses with known weeks in training suggests the presence of bias in training data collection. Training data collection, if not performed prospectively, is subject to uncertainties and may lead to imprecise information on a horse's actual training programme. It is difficult to overcome this challenge as long-term longitudinal studies would be required and trainer motivation to stay in such studies is likely to reduce over time. Finally, we only analysed a small area of subchondral bone of the metacarpal condyles. The use of *ex vivo* micro-CT limits specimen size. Small increases in specimen size increase scan time markedly and further increases in specimen size require the use of an *in vivo* rodent micro-CT or HR-pQCT machine, both of which provide a larger field of view but have the disadvantage of using larger voxel sizes with associated loss of spatial resolution.

Conclusion

We found that age and duration of training had little influence on micromorphology of highly adapted subchondral bone to a depth of 5.1 mm in the area of highest loading in the palmar aspect of the metacarpal condyle in 2 to 4-year-old thoroughbred racehorses. We observed the largest changes in micromorphology in untrained horses between the age of 16 and 20 months and further investigations are required to identify the main drivers for these changes. We also demonstrated that tissue mineral density and bone volume fraction of the seemingly homogeneously sclerotic

subchondral bone changes significantly over 5.1 mm from the articular surface. Further research is needed to elucidate the biomechanical and pathophysiological consequences of these gradients of micromorphological parameters in the subchondral bone.

Acknowledgements

The authors would like to thank David Thomas from the Melbourne Dental School, Faculty of Medicine, Dentistry and Health Sciences, The University of Melbourne, Australia (now retired) for assistance with micro-CT image acquisition, image processing and initial interpretation.

Conflict of Interest

Sandra Martig was supported by an Australian Government Research Training Program Scholarship.

Peta L. Hitchens was supported by a grant from Racing Victoria Limited, Victorian Racing Industry Fund and The University of Melbourne.

The micro-CT examinations were supported with a grant from the ANZ Kathleen Agnes Back Estate.

The authors declare no other financial or competing interests.

Author contributions

S.M. and R.C.W. designed the study. S.M. collected data and conducted preliminary analyses. S.M., M.A.S. and P.L.H. conducted final data analyses and interpretation. R.C.W. provided feedback on data analysis and interpretation. S.M. drafted the manuscript and all authors commented on the manuscript and approved the submitted version.

References

570 **Bani Hassan E, Mirams M, Ghasem-Zadeh A, Mackie EJ, Whitton RC** (2016) Role of subchondral
571 bone remodelling in collapse of the articular surface of Thoroughbred racehorses with
572 palmar osteochondral disease. *Equine Vet. J.* **48**, 228-33.
573 **Barr ED, Pinchbeck GL, Clegg PD, Boyde A, Riggs CM** (2009) Post mortem evaluation of palmar
574 osteochondral disease (traumatic osteochondrosis) of the metacarpo/metatarsophalangeal
575 joint in Thoroughbred racehorses. *Equine Vet. J.* **41**, 366-371.
576 **Bogers SH, Rogers CW, Bolwell CF, et al.** (2014) Impact of race training on volumetric bone mineral
577 density and its spatial distribution in the distal epiphysis of the third metatarsal bone of 2-
578 year-old horses. *Vet. J.* **201**, 353-358.
579 **Boyde A** (2003) The real response of bone to exercise. *J. Anat.* **203**, 173-189.
580 **Boyde A, Firth EC** (2005) Musculoskeletal responses of 2-year-old Thoroughbred horses to early
581 training. 8. Quantitative back-scattered electron scanning electron microscopy and confocal
582 fluorescence microscopy of the epiphysis of the third metacarpal bone. *N. Z. Vet. J.* **53**, 123-
583 132.
584 **Boyde A, Firth EC** (2008) High resolution microscopic survey of third metacarpal articular calcified
585 cartilage and subchondral bone in the juvenile horse: Possible implications in chondro-
586 osseous disease. *Microsc. Res. Tech.* **71**, 477-488.
587 **Boyde A, Haroon Y, Jones SJ, Riggs CM** (1999) Three dimensional structure of the distal condyles of
588 the third metacarpal bone of the horse. *Equine Vet. J.* **31**, 122-129.
589 **Boyde A, Riggs CM, Bushby AJ, et al.** (2011) Cartilage damage involving extrusion of mineralisable
590 matrix from the articular calcified cartilage and subchondral bone. *Eur. Cell. Mater.* **21**, 470-
591 8; discussion 478.
592 **Cogger N, Perkins N, Hodgson DR, Reid SWJ, Evans DL** (2006) Risk factors for musculoskeletal
593 injuries in 2-year-old Thoroughbred racehorses. *Prev. Vet. Med.* **74**, 36-43.
594 **Dykgraaf S, Firth EC, Rogers CW, Kawcak CE** (2008) Effects of exercise on chondrocyte viability and
595 subchondral bone sclerosis in the distal third metacarpal and metatarsal bones of young
596 horses. *Vet. J.* **178**, 53-61.
597 **Fatihhi SJ, Harun MN, Abdul Kadir MR, et al.** (2015) Uniaxial and Multiaxial Fatigue Life Prediction of
598 the Trabecular Bone Based on Physiological Loading: A Comparative Study. *Ann. Biomed.*
599 *Eng.* **43**, 2487-502.
600 **Firth EC, Delahunt J, Wichtel JW, Birch HL, Goodship AE** (1999a) Galloping exercise induces regional
601 changes in bone density within the third and radial carpal bones of Thoroughbred horses.
602 *Equine Vet. J.* **31**, 111-115.

603 **Firth EC, Goodship AE, Delahunt J, Smith T** (1999b) Osteoinductive response in the dorsal aspect of
604 the carpus of young thoroughbreds in training occurs within months. *Equine Vet. J. Suppl.*,
605 552-4.
606 **Firth EC, Rogers CW, Doube M, Jopson NB** (2005) Musculoskeletal responses of 2-year-old
607 Thoroughbred horses to early training. 6. Bone parameters in the third metacarpal and third
608 metatarsal bones. *N. Z. Vet. J.* **53**, 101-112.
609 **Firth EC, Rogers CW, van Weeren PR, et al.** (2011) Mild exercise early in life produces changes in
610 bone size and strength but not density in proximal phalangeal, third metacarpal and third
611 carpal bones of foals. *Vet. J.* **190**, 383-389.
612 **Harrison SM, Whitton RC, Kawcak CE, Stover SM, Pandy MG** (2010) Relationship between muscle
613 forces, joint loading and utilization of elastic strain energy in equine locomotion. *J. Exp. Biol.*
614 **213**, 3998-4009.
615 **Holmes JM, Mirams M, Mackie EJ, Whitton RC** (2014) Thoroughbred horses in race training have
616 lower levels of subchondral bone remodelling in highly loaded regions of the distal
617 metacarpus compared to horses resting from training. *Vet. J.* **202**, 443-447.
618 **Kawcak CE, McIlwraith CW, Firth EC** (2010) Effects of early exercise on metacarpophalangeal joints
619 in horses. *Am. J. Vet. Res.* **71**, 405-411.
620 **Lacourt M, Gao C, Li A, et al.** (2012) Relationship between cartilage and subchondral bone lesions in
621 repetitive impact trauma-induced equine osteoarthritis. *Osteoarthritis Cartilage* **20**, 572-83.
622 **Lambers FM, Koch K, Kuhn G, et al.** (2013) Trabecular bone adapts to long-term cyclic loading by
623 increasing stiffness and normalization of dynamic morphometric rates. *Bone* **55**, 325-34.
624 **Laverty S, Lacourt M, Gao C, Henderson J, Boyde A** (2015) High Density Infill in Cracks and
625 Protrusions from the Articular Calcified Cartilage in Osteoarthritis in Standardbred Horse
626 Carpal Bones. *Int. J. Mol. Sci.* **16**, 9600.
627 **Leahy PD, Smith BS, Easton KL, et al.** (2010) Correlation of mechanical properties within the equine
628 third metacarpal with trabecular bending and multi-density micro-computed tomography
629 data. *Bone* **46**, 1108-1113.
630 **Muir P, Peterson AL, Sample SJ, et al.** (2008) Exercise-induced metacarpophalangeal joint
631 adaptation in the Thoroughbred racehorse. *J. Anat.* **213**, 706-717.
632 **Norrdin RW, Kawcak CE, Capwell BA, McIlwraith CW** (1998) Subchondral bone failure in an equine
633 model of overload arthrosis. *Bone* **22**, 133-139.
634 **Parkin TDH, Clegg PD, French NP, et al.** (2004) Race- and course-level risk factors for fatal distal limb
635 fracture in racing Thoroughbreds. *Equine Vet. J.* **36**, 521-526.

Parkin TDH, Clegg PD, French NP, et al. (2005) Risk factors for fatal lateral condylar fracture of the third metacarpus/metatarsus in UK racing. *Equine Vet. J.* **37**, 192-199.

Pinchbeck GL, Clegg PD, Boyde A, Riggs CM (2013) Pathological and clinical features associated with palmar/plantar osteochondral disease of the metacarpo/metatarsophalangeal joint in Thoroughbred racehorses. *Equine Vet. J.* **45**, 587-592.

Radtke CL, Danova NA, Scollay MC, et al. (2003) Macroscopic changes in the distal ends of the third metacarpal and metatarsal bones of Thoroughbred racehorses with condylar fractures. *Am. J. Vet. Res.* **64**, 1110-1116.

Rapillard L, Charlebois M, Zysset PK (2006) Compressive fatigue behavior of human vertebral trabecular bone. *J. Biomech.* **39**, 2133-2139.

Riggs CM, Boyde A (1999) Effect of exercise on bone density in distal regions of the equine third metacarpal bone in 2-year-old thoroughbreds. *Equine Vet. J. Suppl.* **S30**, 555-60.

Riggs CM, Whitehouse GH, Boyde A (1999a) Pathology of the distal condyles of the third metacarpal and third metatarsal bones of the horse. *Equine Vet. J.* **31**, 140-148.

Riggs CM, Whitehouse GH, Boyde A (1999b) Structural variation of the distal condyles of the third metacarpal and third metatarsal bones in the horse. *Equine Vet. J.* **31**, 130-139.

Rubio-Martinez LM, Cruz AM, Gordon K, Hurtig MB (2008) Structural characterization of subchondral bone in the distal aspect of third metacarpal bones from Thoroughbred racehorses via micro-computed tomography. *Am. J. Vet. Res.* **69**, 1413-1422.

Senat (1991) Aspects of animal welfare in the racing industry. (ed welfare Sscoa), pp. 11-18. Canberra: Commonwealth of Australia.

Stepnik MW, Radtke CL, Scollay MC, et al. (2004) Scanning electron microscopic examination of third metacarpal/third metatarsal bone failure surfaces in thoroughbred racehorses with condylar fracture. *Vet. Surg.* **33**, 2-10.

Trope GD, Anderson GA, Whitton RC (2011) Patterns of scintigraphic uptake in the fetlock joint of Thoroughbred racehorses and the effect of increased radiopharmaceutical uptake in the distal metacarpal/tarsal condyle on performance. *Equine Vet. J.* **43**, 509-15.

Tull TM, Bramlage LR (2011) Racing prognosis after cumulative stress-induced injury of the distal portion of the third metacarpal and third metatarsal bones in Thoroughbred racehorses: 55 cases (2000-2009). *J. Am. Vet. Med. Assoc.* **238**, 1316-1322.

Turley SM, Thambyah A, Riggs CM, Firth EC, Broom ND (2014) Microstructural changes in cartilage and bone related to repetitive overloading in an equine athlete model. *J. Anat.* **224**, 647-658.

Verheyen K, Price J, Lanyon L, Wood J (2006) Exercise distance and speed affect the risk of fracture in racehorses. *Bone* **39**, 1322-1330.

White J, Yeats A, Skipworth G (1977) Tables for statisticians. In *Tables for statisticians*), pp. 36-37. St.Lucia, Queensland: University of Queensland Press.

Whitton RC, Mirams M, Mackie EJ, Anderson GA, Seeman E (2013) Exercise-induced inhibition of remodelling is focally offset with fatigue fracture in racehorses. *Osteoporos. Int.* **24**, 2043-2048.

Whitton RC, Trope GD, Ghasem-Zadeh A, et al. (2010) Third metacarpal condylar fatigue fractures in equine athletes occur within previously modelled subchondral bone. *Bone* **47**, 826-831.

Williamson AJ, Sims NA, Thomas CDL, et al. (2017) Biomechanical testing of the calcified metacarpal articular surface and its association with subchondral bone microstructure in Thoroughbred racehorses. *Equine Vet. J.* 10.1111/evj.12748.

682 **Table 1**: Mean and standard deviation of micro-CT parameters of a subchondral bone sample from the palmar aspect of the lateral metacarpal
683 condyle in untrained and trained thoroughbred racehorses.

	VOI	BV/TV (%)	lBV/TV (%)	hBV/TV (%)	TMD (g/cm^3)	lTMD (g/cm^3)	hTMD (g/cm^3)	clporestra	aclporestra (mm^2)	BS/TV (mm^{-1})	BS/BV (mm^{-1})
Untrained horses											
All	prox	76.4 ± 9.9	25.4 ± 9.3	50.9 ± 1.3	1.06 ± 0.03	0.92 ± 0.04	1.13 ± 0.04	289 ± 58	4.10 ± 1.81	7.76 ± 0.76	10.30 ± 2.26
untrained	mid	82.3 ± 10.4	32.1 ± 10.8	50.2 ± 2.0	1.01 ± 0.03	0.89 ± 0.04	1.08 ± 0.04	355 ± 93	2.97 ± 1.96	7.60 ± 1.14	9.53 ± 2.68
(n = 9)	dist	87.4 ± 9.9	38.0 ± 11.3	49.3 ± 2.5	0.90 ± 0.03	0.78 ± 0.05	0.99 ± 0.05	417 ± 82	2.39 ± 1.82	7.50 ± 2.46	8.98 ± 3.97
1-year-old	prox	69.8 ± 9.7	19.0 ± 8.7	50.7 ± 1.2	1.05 ± 0.02	0.90 ± 0.04	1.11 ± 0.04	268 ± 59	5.31 ± 1.70	8.18 ± 0.44	11.93 ± 2.09
(n = 4)	mid	74.1 ± 10.1	23.1 ± 9.4	50.9 ± 2.8	1.00 ± 0.03	0.86 ± 0.05	1.06 ± 0.04	283 ± 96	4.57 ± 1.87	8.52 ± 0.77	11.74 ± 2.35
	dist	78.4 ±7.5	28.0 ± 8.5	50.3 ± 2.7	0.88 ± 0.03	0.75 ± 0.04	0.96 ± 0.05	424 ± 75	4.04 ± 1.13	9.68 ± 1.26	12.53 ± 2.70
2-year-old	prox	81.7 ± 6.8	30.6 ± 6.5	51.1 ± 1.5	1.06 ± 0.03	0.93 ± 0.04	1.14 ± 0.04	307 ± 56	3.14 ± 1.32	7.27 ± 0.73	8.99 ± 1.45
(n = 5)	mid	88.9 ±4.6	39.2 ± 4.9	49.6 ± 1.2	1.01 ± 0.03	0.91 ± 0.03	1.10 ± 0.03	413 ± 32	1.68 ± 0.66	6.86 ± 0.79	7.76 ± 1.22
	dist	94.5 ± 3.1	46.0 ± 4.5	48.6 ± 2.2	0.91 ± 0.03	0.81 ± 0.02	1.01 ± 0.04	412 ± 96	1.08 ± 0.87	5.76 ± 1.55	6.15 ± 1.86
Trained horses											
2-year-old	prox	87.7 ± 4.8	36.5 ± 6.2	51.2 ± 2.0	1.08 ± 0.04	0.95 ± 0.04	1.16 ± 0.04	386 ± 56	2.03 ± 0.81	6.73 ± 0.65	7.73 ± 1.11
(n = 14)	mid	93.7 ± 2.7	43.6 ± 3.5	50.1 ± 1.6	1.03 ± 0.04	0.92 ± 0.04	1.12 ± 0.04	413 ± 55	0.92 ± 0.38	5.86 ± 0.86	6.29 ± 1.09
	dist	97.0 ± 1.4	55.1 ± 6.9	41.9 ± 5.7	0.92 ± 0.03	0.84 ± 0.03	1.04 ± 0.04	399 ± 67	0.56 ± 0.38	4.79 ± 0.85	4.95 ± 0.95
3-year-old	prox	88.3 ± 7.3	37.6 ± 7.9	50.7 ± 1.4	1.06 ± 0.05	0.94 ± 0.05	1.15 ± 0.05	378 ± 73	1.93 ± 1.20	6.44 ± 0.93	7.42 ± 1.69
(n = 15)	mid	93.1 ± 4.2	42.7 ± 4.6	50.3 ± 1.8	1.02 ± 0.05	0.91 ± 0.05	1.11 ± 0.06	361 ± 64	1.11 ± 0.69	5.73 ± 1.04	6.21 ± 1.40
	dist	96.3 ± 2.5	53.8 ± 7.9	42.4 ± 6.0	0.93 ± 0.04	0.84 ± 0.04	1.04 ± 0.05	410 ± 112	0.58 ± 0.47	5.09 ± 1.51	5.33 ± 1.74
4-year-old	prox	91.8 ± 4.9	40.3 ± 6.0	51.5 ± 2.1	1.08 ± 0.03	0.96 ± 0.03	1.17 ± 0.03	441 ± 118	1.41 ± 0.79	6.11 ± 1.22	6.72 ± 1.60
(n = 11)	mid	94.1 ± 3.5	44.4 ± 4.3	49.7 ± 1.4	1.02 ± 0.03	0.92 ± 0.04	1.12 ± 0.04	412 ± 116	1.12 ± 0.69	5.69 ± 1.47	6.11 ± 1.81
	dist	96.0 ± 1.8	50.3 ± 6.3	45.7 ± 4.8	0.93 ± 0.02	0.83 ± 0.03	1.03 ± 0.03	462 ± 106	0.71 ± 0.33	5.39 ± 1.13	5.64 ± 1.29

684 VOI: volume of interest (5.3 mm in diameter and 1.7 mm in height); prox: proximal; mid: middle; dist: distal (includes articular surface); BV/TV: bone volume
685 fraction; lBV/TV: volume fraction of less mineralised bone; hBV/TV: volume fraction of highly mineralised bone; TMD: tissue mineral density of all mineralised
686 tissue; lTMD: tissue mineral density of less mineralised tissue; hTMD: tissue mineral density of highly mineralised tissue; clporestra: number of closed pores

on cross-section (average of 100 slices); aclporestra: area of closed pores in cross-section (average of 100 slices); BS/TV: bone surface density; BS/BV: specific bone surface; yo: year-old.

Table 2: Estimated coefficients from multivariable mixed-effects linear regression models of factors affecting total bone volume fraction, bone volume fraction of highly mineralized bone, tissue mineral density and number of closed pores in cross-section in the palmar aspect of the lateral metacarpal condyle in forty 2, 3 and 4 year-old thoroughbred racehorses in training.

Variable	BV/TV		hBV/TV		TMD		clporestra	
	Coef (95% CI)	p-value	Coef (95% CI)	p-value	Coef (95% CI)	p-value	Coef (95% CI)	p-value
intercept	96.4 (95.2 to 97.7)	<0.001	42.0 (40.8 to 43.2)	<0.001	0.93 (0.91 to 0.95)	<0.001	387 (365 to 408)	<0.001
VOI:								
distal	reference		reference		reference			
middle	-2.9 (-4.4 to -1.4)	<0.001	8.1 (6.4 to 9.8)[b]	<0.001	0.10 (0.09 to 0.10)	<0.001		
proximal	-7.4 (-8.9 to -5.9)	<0.001	9.2 (7.5 to 10.9)	<0.001	0.15 (0.14 to 0.15)	<0.001		
weeks in training:								
known					reference			
unknown					-0.04 (-0.07 to -0.02)	0.001		
euthanasia					0.02 (-0.001 to 0.04)	0.051		
SCBI			5.2 (2.7 to 7.7)	<0.001			77 (31 to 123)	<0.001
SCBI#VOI								
SCBI distal			reference					
SCBI middle			-5.3 (-8.9 to -1.8)	0.003				
SCBI proximal			-5.5 (-9.0 to -2.0)	0.002				
random effects[a]								

horse	2.4 (1.6 to 3.5)	<0.001		0.03 (0.02 to 0.04)	<0.001	47 (32 to 70)	<0.001

# Denotes interaction between SCB and VOI. [a] Variance of the random effect term. There was no horse level (random) effect for bone volume fraction of highly mineralized bone (P = 1.0). [b] The estimated bone volume fraction of highly mineralized bone in the middle VOI is 8.1 % higher (95% confidence interval 6.4 to 9.8) than in the distal VOI if all other variables are kept unchanged. VOI: volume of interest (5.3 mm in diameter and 1.7 mm in height, distal VOI slightly smaller as includes curved articular surface); BV/TV: bone volume fraction; hBV/TV: volume fraction of highly mineralised bone; TMD: average tissue mineral density of all mineralised tissue; clporestra: number of closed pores on cross-section (average of 100 slices); SCBI: subchondral bone injury; euthanasia: euthanized because of musculoskeletal stress injury.

698 **Figure legends**

699 **Fig. 1:** Surface rendering of clinical computed tomography images of the palmar aspect of the distal
700 metacarpal condyles of the right limb of a 5-year-old Thoroughbred racehorse demonstrating
701 sampling location of the bone cores used for this study. (a) long axis of metacarpal bone, (b) line of
702 cut to collect palmar aspect of the metacarpal condyles, the angle alpha between lines (a) and (b) is
703 55°. The black oval indicates the location of the extracted bone core with the long axis of the bone
704 core being at approximately 90° to line (b).

705 **Fig. 2:** Biplot of micro-CT parameters of equine subchondral bone assessed in three consecutive
706 volumes of interest (VOI, 5.3 mm in diameter, 1.7 mm in length). The directed arrows represent the
707 variables and how closely they are correlated with each other. The points represent each observation,
708 stratified by VOI. Their location is approximated using the scores of the observations on the first two
709 principal components. Two of the measures of the amount of bone volume fraction (bvtv: bone
710 volume fraction, lbvtv: bone volume fraction of less mineralized bone) are positively correlated with
711 each other and negatively correlated with measures of bone surface (aclporestra: area of closed
712 pores in cross-section, bsdens: bone surface density, sbs: specific bone surface) and form
713 component 1 of PCA. Measures of tissue mineral density cluster together in the biplot and form
714 component 2 in PCA (tmd: tissue mineral density, htmd: mineral density of highly mineralized tissue,
715 ltmd: mineral density of less mineralized tissue). ltmd and htmd are superimposed with each other
716 indicating they are colinear. Component 3 from PCA consists of the remaining bone volume fraction
717 measure (hbvtv: bone volume fraction of highly mineralized bone), as well as number of closed pores
718 in cross-section (clporestra) and bsdens (which loads stronger in component 3 than in component 1).
719 Note the clustering of VOIs indicating changing micromorphology with increasing distance from the
720 articular surface.

721 **Fig. 3:** Unfiltered dorsal plane single slice micro-CT images (4.7 µm nominal pixel size) of
722 subchondral bone from the palmar aspect of the lateral metacarpal condyle from thoroughbred
723 racehorses. The images have been rotated to align the long axis of the specimen vertically. The
724 articular surface is at the top. A: untrained 1-year-old, B: untrained 2-year-old, C: trained 2-year-old,
725 D: trained 3-year-old, E: trained 4-year-old. The bar is 1 mm long.

726 **Fig. 4:** Unfiltered dorsal (top) and transverse plane (bottom) micro-CT images (4.7 µm nominal pixel
727 size) of the subchondral bone in the palmar aspect of lateral metacarpal condyle from thoroughbred
728 racehorses in training. In dorsal plane images the articular surface is at the top. A: high-density line at
729 the articular surface in a 2-year-old without subchondral bone injury; the uneven shape of the
730 transverse image is due to the curved articular surface, B: microcracks in a 3-year-old with
731 subchondral bone injury, C: a cluster of large pores is present in a band parallel to the articular
732 surface in a 3-year-old without subchondral bone injury.

733 **Fig. 5:** Predicted margins of bone volume fraction of highly mineralized bone with 95% confidence
734 intervals as a function of subchondral bone injury (SCBI). Horses with SCBI had a higher amount of

highly mineralised bone in the distal volume of interest than horses without SCBI (interaction effect P = 0.003). No differences were observed in the middle and proximal volumes of interest. Volume of interest (5.3 mm in diameter, 1.7 mm in length): 1: distal; 2: middle; 3: proximal.

Fig. 6: Scatter plot of tissue mineral density as a function of bone volume fraction with linear regression line for each volume of interest (VOI, 5.3 mm in diameter, 1.7 mm in length). The linear correlation was only statistically significant in the distal VOI (circles, dashed line): tissue mineral density = 0.12 + 0.008 x bone volume fraction, R^2 = 0.30, P < 0.001, 95% CI -0.29 to 0.52 (intercept) and 0.004 to 0.013 (coefficient) but not in the middle (P = 0.17, triangles, solid line) and proximal VOIs (P = 0.8, squares, dotted line).

Fig. 7: Scatter plot of number of closed pores in cross-section (clporestra) as a function of area of closed pores in cross-section (aclporestra) with regression lines for each volume of interest (VOI, 5.3 mm in diameter, 1.7 mm in length). Distal VOI (circles, dashed line): clporestra = 304 + 192 x aclporestra, R^2 = 0.61, P < 0.001, 95% CI 267 to 340 (intercept) and 141 to 242 (coefficient). Proximal VOI (squares, dotted line): clporestra = 469 - 39 x aclporestra, R^2 0.20, P = 0.004, 95% CI 416 to 522 (intercept) and -65 to -13 (coefficient). The linear relationship between number and area of closed pores in cross-section was not statistically significant in the middle VOI (P = 0.051, triangles, solid line).

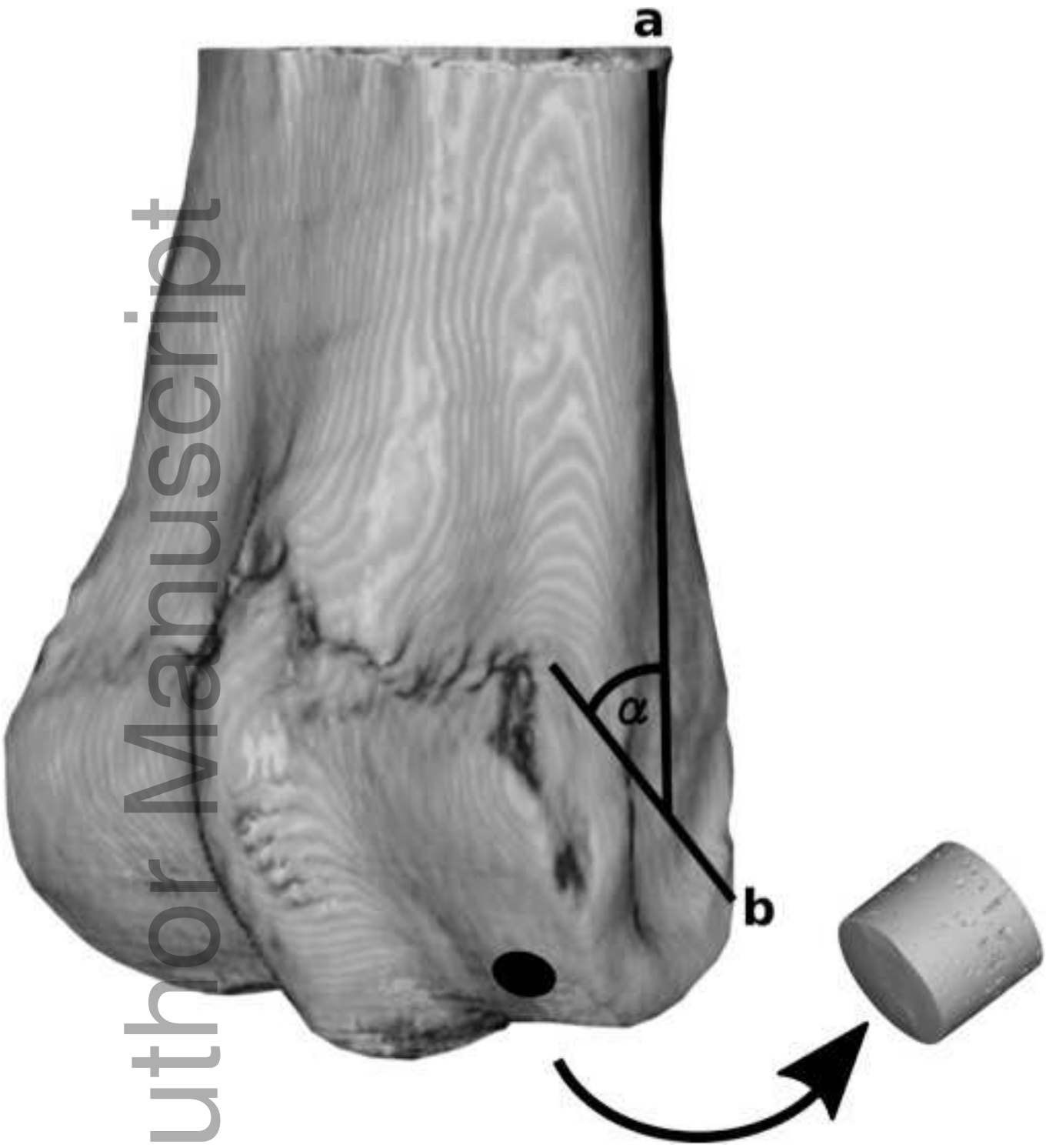

joa_12794_f1.tif

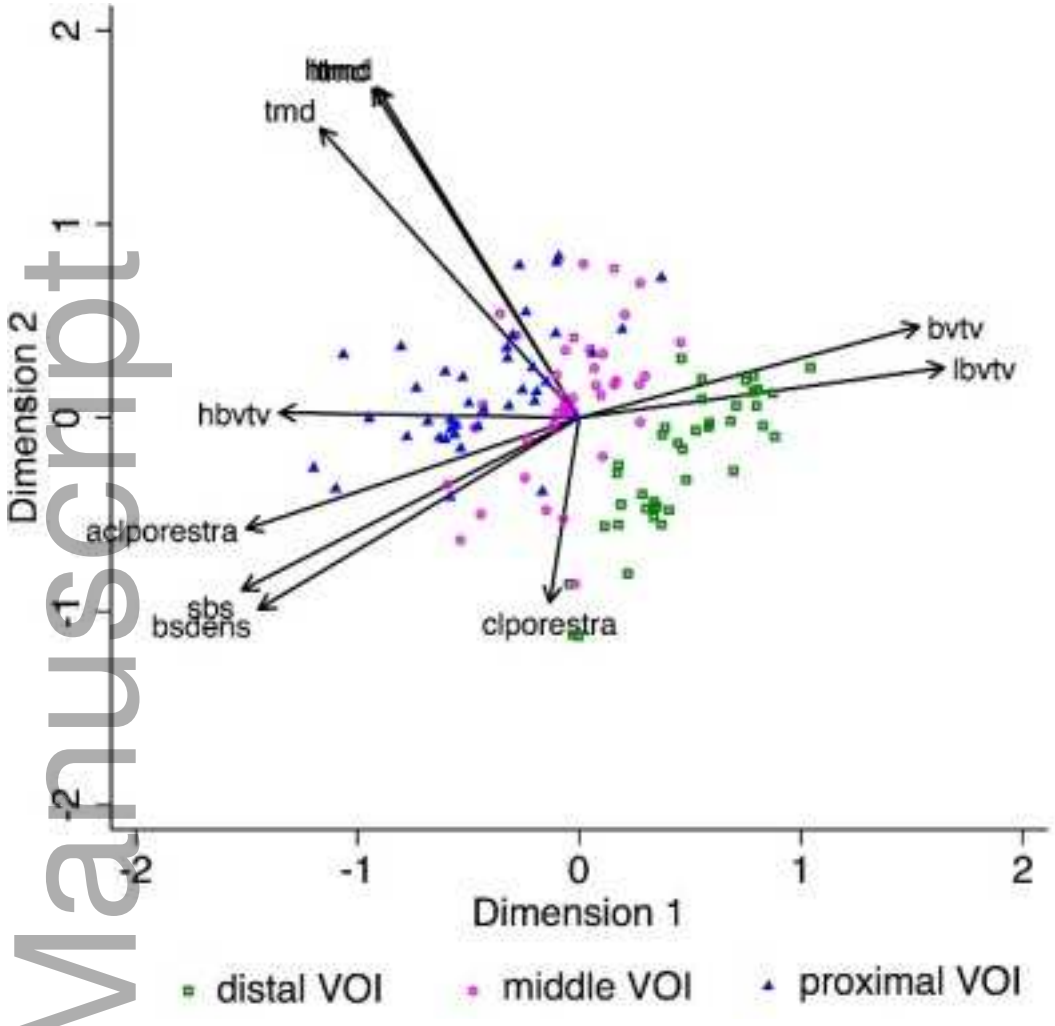

joa_12794_f2.tif

joa_12794_f3.tif

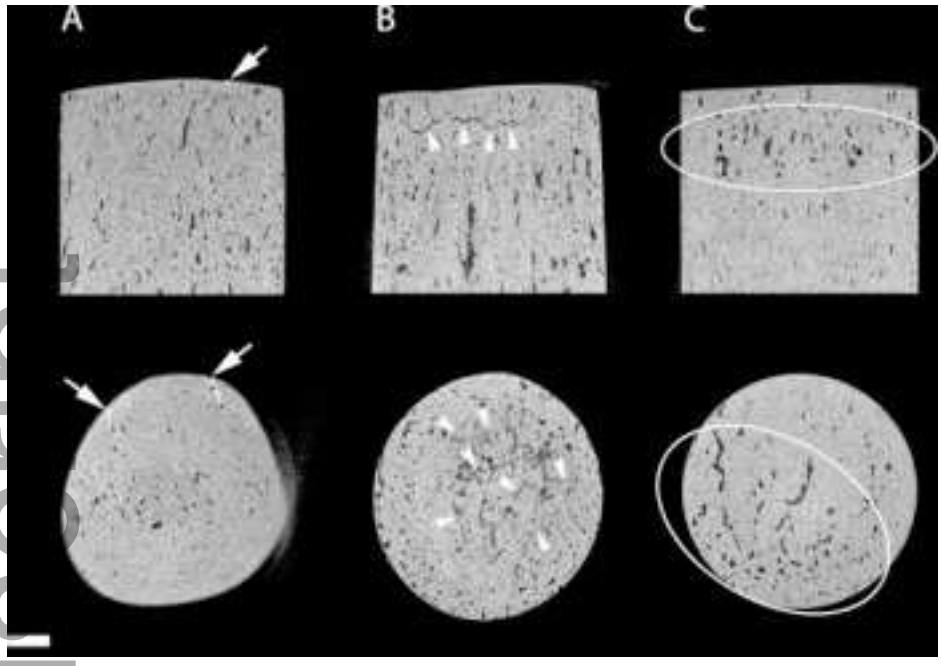

joa_12794_f4.tif

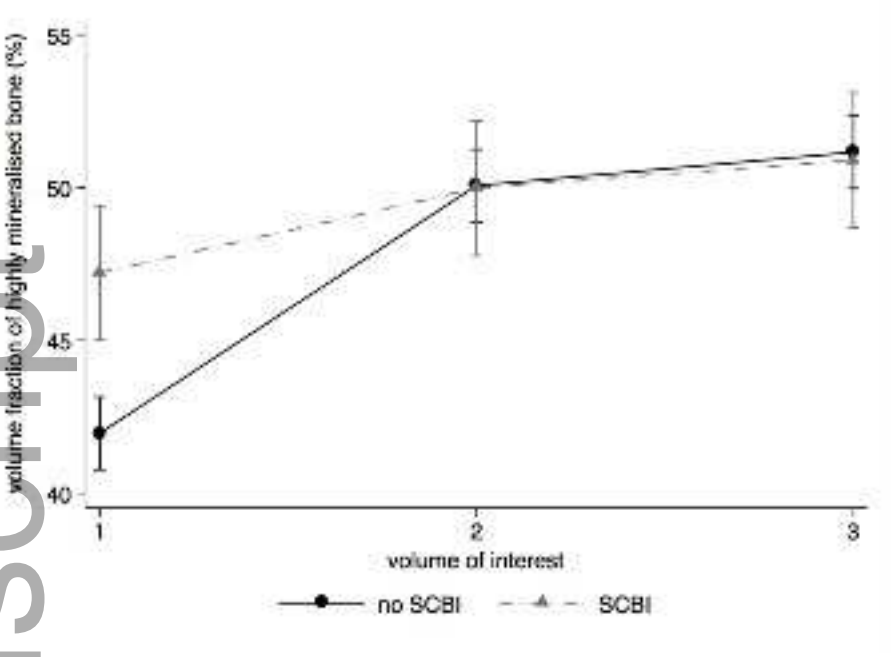

joa_12794_f5.tif

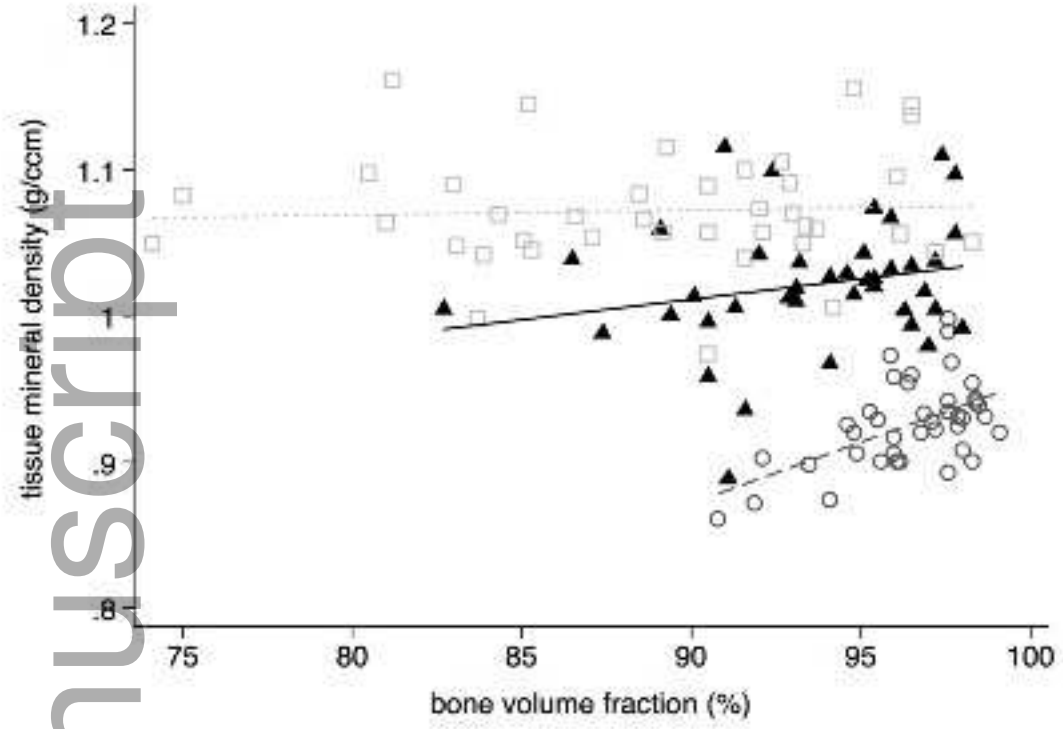

joa_12794_f6.tif

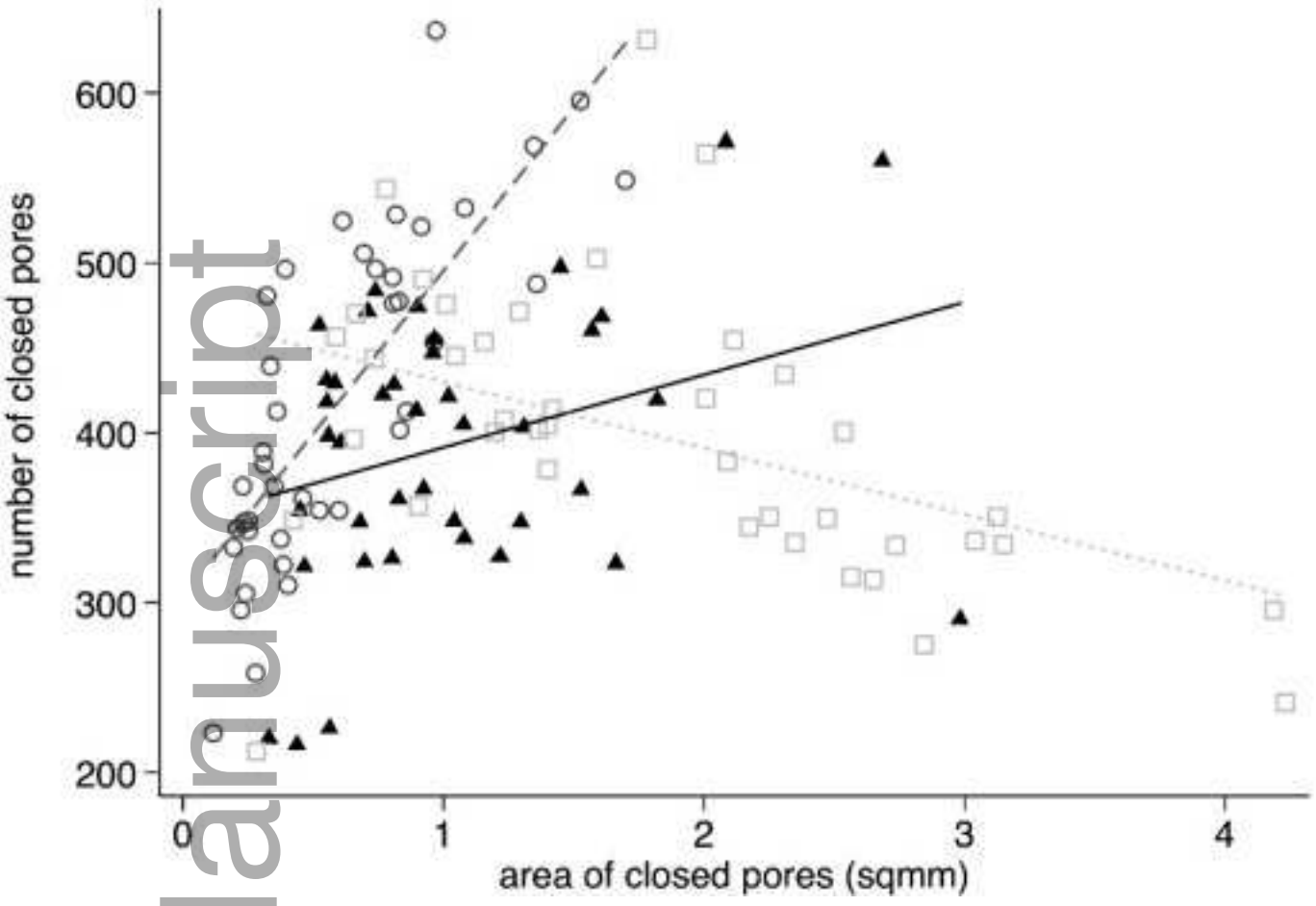

joa_12794_f7.tif